g-factor and spin-parity assignments of excited states in the $N = 83$ isotones ^{135}Te, ^{136}I, ^{137}Xe, and ^{138}Cs

S. H. Liu,[1] J. H. Hamilton,[1] A. V. Ramayya,[1] A. Covello,[2,3] A. Gargano,[3] N. Itaco,[2,3] N. J. Stone,[4,5] A. V. Daniel,[1,6] J. K. Hwang,[1] Y. X. Luo,[1,7] J. O. Rasmussen,[7] G. M. Ter-Akopian,[6] S. J. Zhu,[8] and W. C. Ma[9]

[1]*Department of Physics and Astronomy, Vanderbilt University, Nashville, Tennessee 37235, USA*
[2]*Dipartimento di Scienze Fisiche, Complesso Universitario di Monte San Angelo, Via Cintia, I-80126 Naples, Italy*
[3]*Istituto Nazionale di Fisica Nucleare, Complesso Universitario di Monte San Angelo, Via Cintia, I-80126 Naples, Italy*
[4]*Department of Physics, Oxford University, Oxford OX1 3PU, United Kingdom*
[5]*Department of Physics and Astronomy, University of Tennessee, Knoxville, Tennessee 37996, USA*
[6]*Flerov Laboratory of Nuclear Reactions, Joint Institute for Nuclear Research, RU-141980 Moscow Region, Dubna, Russia*
[7]*Lawrence Berkeley National Laboratory, Berkeley, California 94720, USA*
[8]*Department of Physics, Tsinghua University, Beijing 100084, People's Republic of China*
[9]*Department of Physics and Astronomy, Mississippi State University, Mississippi State, Mississippi 39762, USA*

(Received 1 December 2009; published 29 January 2010)

The g factor of the $15/2^-$ state in ^{137}Xe was measured for the first time by using a newly developed technique for measuring angular correlations with Gammasphere. Spins and parities were assigned to several levels in the $N = 83$ isotones ^{135}Te, ^{136}I, ^{137}Xe, and ^{138}Cs. The calculated g factor in the shell-model frame is in good agreement with the measured one in the present work. Shell-model calculations also support our spin-parity assignments.

DOI: 10.1103/PhysRevC.81.014316 PACS number(s): 21.10.Ky, 21.60.Cs, 25.85.Ca, 27.60.+j

I. INTRODUCTION

The study of nuclei with several valence nucleons beyond the doubly magic core ^{132}Sn is a subject of special interest. In particular, the magnetic moments of such nuclei provide direct insight into the single-particle structure of the orbitals outside the major shells. The g factor is also sensitive to the two-body interactions of the valence particles and their interactions with the core. Therefore measurements of g factors of excited states in isotopes near the doubly magic ^{132}Sn core help us to understand nuclear shell structure in this region. Moreover, spin-parity assignments of excited states in these nuclei provide important tests of shell-model calculations. The previously unknown g factor of the $15/2^-$ state in ^{137}Xe is measured in this article using a newly developed technique to perform angular correlation measurements with Gammasphere [1]. The experimental g factor is reproduced very well by shell-model calculations with a two-body effective interaction derived from the CD-Bonn nucleon-nucleon potential. In addition, the measured angular correlation coefficients are used to assign and confirm spins and parities of several levels in ^{135}Te, ^{136}I, ^{137}Xe, and ^{138}Cs, which are also supported by shell-model calculations reported here.

II. EXPERIMENTAL DATA ANALYSIS

The data for the present angular correlation measurements were obtained using the Gammasphere detector array with 101 detectors at Lawrence Berkeley National Laboratory. A ^{252}Cf spontaneous fission source with an α activity of 62 μCi was sandwiched between two 10 mg/cm^2 iron foils, which were used to stop the fission fragments and eliminate the need for a Doppler correction. A total of 5.7×10^{11} triple- and higher-fold γ-ray coincidence events were measured. More details about this experiment and data analysis procedure can be found in Ref. [2]. A newly developed technique for measuring angular correlations with the Gammasphere detector array by sorting our high statistics data into 17 angle bins was used here to measure the g factor of and assign spins and parities to excited states in neutron-rich nuclei produced in the spontaneous fission of ^{252}Cf. More details of this technique can be found in Ref. [1].

As mentioned earlier, the fission fragments were implanted and stopped in a ferromagnetic material (the iron foils), where they were subjected to the hyperfine fields (B_{HF}) caused by their implantation in substitutional sites in the iron lattice. It becomes possible for us to carry out angular correlation measurements to determine the spins and parities of levels and the g factors of long-lived states using the integral perturbed angular correlation (IPAC) technique [3]. For an intermediate nuclear state with a lifetime τ, the spin vector of this nucleus will rotate about B_{HF} over the lifetime of the state, with a rotational frequency proportional to the strength of the field and the g factor of the state. For our experiment, the magnetic domains in the iron foils, which were not cooled and not affected by any external field, remained randomly oriented. Then the net result of the rotation of the implanted nucleus about the randomly oriented hyperfine fields (B_{HF}) is an attenuation of the expected angular correlation. This is the basic idea of the IPAC technique for g-factor measurement.

The attenuation factor G_k is related to the Larmor precession frequency ω_L and the lifetime τ by [4]

$$G_k = \frac{1}{2k+1}\left(1 + 2\sum_{q>0}^{k} \frac{1}{1+q^2\phi^2}\right), \tag{1}$$

where the Larmor precession frequency ω_L is given by

$$\omega_L = \frac{\phi}{\tau} = -\frac{\mu_N g B_{\mathrm{HF}}}{\hbar}. \tag{2}$$

In these equations, g is the nuclear g factor, $B_{\rm HF}$ is the nuclear hyperfine field in iron, and μ_N is the nuclear magneton. If the lifetime of the state that interacts with $B_{\rm HF}$s is much longer than the stopping time (a few picoseconds), the attenuation will be measurable. Here attenuation implies that the absolute measured values of the angular correlation coefficients will decrease. Therefore the angular correlation function $W(\theta)$ becomes

$$W(\theta) = 1 + A_2^{\rm theory}(\delta)G_2 P_2(\cos\theta) + A_4^{\rm theory}(\delta)G_4 P_4(\cos\theta), \quad (3)$$

where G_2 and G_4 are the preceding attenuation factors, defined as

$$G_k = \frac{A_k^{\rm exp}(\delta)}{A_k^{\rm theory}(\delta)}. \quad (4)$$

The $A_{2,4}^{\rm theory}$ can be calculated for various values of the mixing ratio, δ, with the Wigner 3-j and 6-j coefficients, as outlined and tabulated in Refs. [5,6]. With these theoretical values, the attenuation factor G_k is found by measuring $A_k^{\rm exp}$ and then using Eq. (4). The g factor of the state can be extracted by solving Eqs. (1) and (2) as

$$g = -\frac{\hbar\phi}{\mu_N B_{\rm HF}\tau}. \quad (5)$$

It is worth noting that ϕ, proportional to the product $gB_{\rm HF}\tau$, needs to be within certain limits for the present method to be applicable. If ϕ is very small, the angular correlation will not be attenuated; if ϕ is quite large, then the G_ks will approach their asymptotic limits of $G_2 = 1/5$ and $G_4 = 1/9$, respectively, as indicated in Eq. (1), with no useful information for the g-factor measurements.

In iron, hyperfine fields are of an order between 10 and 100 T, and typically, g factors for states with lifetimes between a few hundred picoseconds and a few nanoseconds can be measured by IPAC with the source/foil arrangement used in this article. For the excited states with a very short lifetime, but still longer than the stopping time, it is assumed that the angular correlations will not be perturbed and that no attenuation will be observed. To obtain the nuclear g factor from the angular correlation attenuation, the hyperfine field needs to be known. Our previous reports on this method [7–9] showed that the hyperfine fields were not aligned and that no significant electric fields were generated by radiation damage in the foils. The compilation by Rao [10] is a useful, though somewhat outdated, source of the $B_{\rm HF}$ values. The adopted values for this article will be discussed in the next section.

Because only ϕ^2 can be obtained from Eq. (1), our method can measure the magnitude, but not the sign, of the g factor. Because of the extremely high statistics of our experimental data, some additional coincidence gates can be applied to the angular correlation of interest for better selectivity. In this article, it is not necessary to use additional gates in some cases because the γ-γ coincidence spectrum is relatively clean for transitions of energies >1 MeV. Moreover, most of the correlations here are unattenuated because of large transition energies for the $N = 83$ isotones.

More details about this method, in particular regarding the solid-angle correction, binning of the data, and relative detector efficiencies at Gammasphere, can be found in Ref. [1].

III. RESULTS

Figure 1 shows the partial level schemes of ^{135}Te, ^{136}I, ^{137}Xe, and ^{138}Cs, where data are taken from Refs. [2,11–16] and the present work. The spins and parities given to some of the states are determined by the angular correlations measured here. The details of the assignments for levels and the measurement of the g factor of the $15/2^-$ state in ^{137}Xe will be discussed later. The results of the angular correlations in the present work are summarized in Table I.

For ^{135}Te, the measured A_2 and A_4 for the $325.0 \to 1180.3$ keV cascade are 0.097(6) and 0.007(9), respectively, which are obtained from the angular correlation shown in Fig. 2. The A_2 and A_4 here are consistent with the theoretical values 0.102 and 0.009 for a pure quadrupole $\to$ quadrupole cascade. Because of the yrast feature and high spin character of the 1180.3 and 1505.3 keV levels, these two transitions are of $E2$ character. Then, with the known spin and parity of the

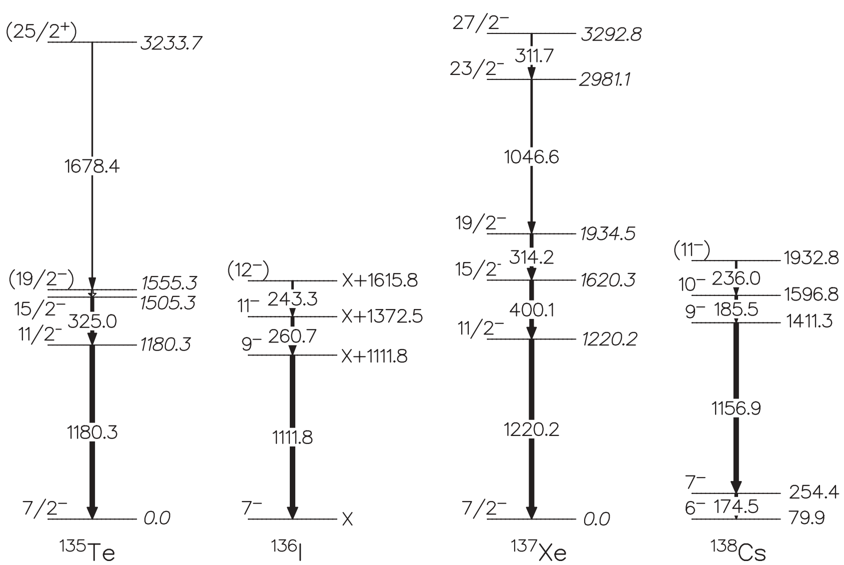

FIG. 1. Partial level scheme of ^{135}Te, ^{136}I, ^{137}Xe, and ^{138}Cs with spins and parities assigned in this work. Data are taken from Refs. [2,11–16] and the present work.

TABLE I. Angular correlations measured in the present work. A_2^{theory} and A_4^{theory} of γ-γ angular correlations for a pure quadrupole-quadrupole cascade are indicated. The additional gates used for better selectivity are listed as well.

Nucleus	Cascade (keV)	Spin sequence	A_2^{exp}, A_4^{exp}	A_2^{theory}, A_4^{theory}	Additional gates (keV)
^{135}Te	325.0 → 1180.3	$15/2^- \to 11/2^- \to 7/2^-$	0.097(6), 0.007(9)	0.102, 0.009	None
^{136}I	260.7 → 1111.8	$11^- \to 9^- \to 7^-$	0.101(6), 0.009(10)	0.102, 0.009	None
^{137}Xe	4001 → 1220.2	$15/2^- \to 11/2^- \to 7/2^-$	0.103(5), 0.012(8)	0.102, 0.009	314.2, 1046.6, 311.7, 1091.5, 240.8, 422.3, 150.4, 236.6
	314.2 → 400.1	$19/2^- \to 15/2^- \to 11/2^-$	0.072(7), 0.014(10)	0.102, 0.009	None
	311.7 → 1046.6	$27/2^- \to 23/2^- \to 19/2^-$	0.091(13), 0.009(19)	0.102, 0.009	1200.2, 400.1, 314.2, 1091.5, 304.9, 240.8, 150.4, 236.6
^{138}Cs	185.5 → 1156.9	$10^- \to 9^- \to 7^-$	−0.076(23), −0.007(34)	−0.071, 0.0	174.5, 236.0, 84.7, 895.5, 137.3, 222.0

ground state as $7/2^-$, the spins and parities of the 1180.3 and 1505.3 keV levels are assigned as $11/2^-$ and $15/2^-$, respectively, which agrees with the previous shell-model predictions [11,12,17].

For ^{136}I, the measured A_2 and A_4 for the $260.7 \to 1111.8$ keV cascade are 0.101(6) and 0.009(10), respectively, which are obtained from the angular correlation shown in Fig. 3. The A_2 and A_4 values here are consistent with the theoretical ones of $A_2 = 0.102$ and $A_4 = 0.009$ for a pure quadrupole → quadrupole cascade. Because the high spin states in ^{136}I were proposed to be built on the 7^- isomeric state [11,13], 9^- and 11^- are assigned to the $X + 1111.8$ and $X + 1372.5$ keV levels, respectively, which confirms the previously calculated results in the shell-model frame [11,17].

For ^{137}Xe, the measured A_2 and A_4 for the $400.1 \to 1220.2$ keV cascade are 0.103(5) and 0.012(8), respectively, which are obtained from the angular correlation shown in Fig. 4. These values are consistent with $A_2^{\text{theory}} = 0.102$ and $A_4^{\text{theory}} = 0.009$ for a pure quadrupole → quadrupole cascade, which indicates that the $15/2^- \to 11/2^- \to 7/2^-$ cascade is unattenuated. However, an attenuation seems to occur in the angular correlation of the $314.2 \to 400.1$ keV cascade, as presented in Fig. 5, because the spin-parity sequence of $19/2^- \to 15/2^- \to 11/2^-$ was firmly assigned to this cascade in experiment [14] and theory [17], and the multipolarities of these two transitions were determined as $E2$ [14]. To extract the g factor from the attenuation, the hyperfine field acting on the nucleus and the lifetime of the state must be known. The comprehensive hyperfine field compilation in Ref. [10] provides a wide range of fields for Xe in the iron host for samples with different preparation methods and at different temperatures. As was discussed in our previous article [8], we adopt the B_{HF}(Xe) value as 73(8) T given in Ref. [10]. The g factors in heavier Xe isotopes extracted using $B_{\text{HF}}(\text{Xe}) = 73(8)$ T were predicted by Interacting Boson Model-2 (IBM-2) very well in Ref. [8]. There is no measured value of the lifetime of the $15/2^-$ level. As in our previous article regarding the g factor of the $15/2^+$ state in ^{135}I [7], shell-model calculations are used to obtain the lifetime of the $15/2^-$ state in ^{137}Xe. The lifetime of the $15/2^-$ state is calculated to be 0.6 ns. The details of the calculations will be presented in the following section. Thus, with the measured attenuation factor $G_2 = 0.71(7)$, the g factor of the $15/2^-$ state in ^{137}Xe is obtained as 0.26(5) using Eqs. (1) and (5).

For the spin-parity assignment of the 2981.1 keV level in ^{137}Xe, one can use the correlation of the $1046.6 \to 314.2$ keV cascade because the multipolarity of the 314.2 keV transition is known to be $E2$ [14]. However, the 1934.5 keV ($19/2^-$) level has a lifetime of 11.7(6) ns [18], which makes the angular correlation of the $1046.6 \to 314.2$ keV cascade heavily attenuated. Then we choose the $311.7 \to 1046.6$ keV cascade and measure the correlation between these two transitions to determine the multipolarity of the 1046.6 keV transition because the 311.7 keV transition is known to have an $E2$ character from linear polarization measurements [14]. The correlation shown in Fig. 6 gives the A_2 and A_4 values as 0.091(13) and 0.009(19), respectively. These values are in good agreement with theory for a pure quadrupole → quadrupole cascade. On the basis

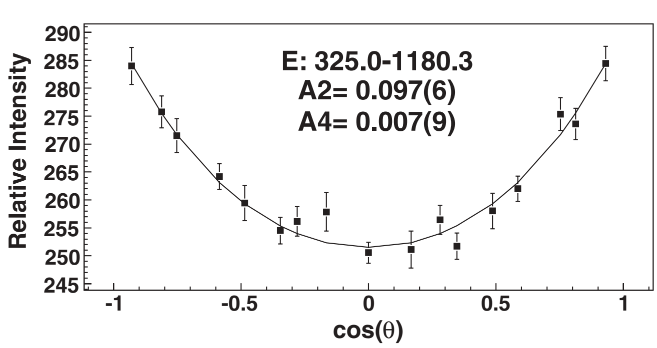

FIG. 2. Angular correlation for the $325.0 \to 1180.3$ keV cascade in ^{135}Te.

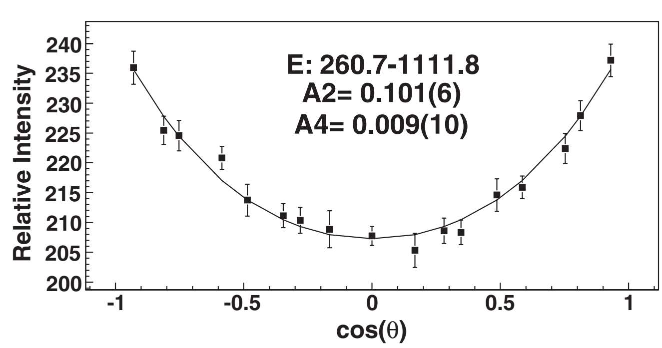

FIG. 3. Angular correlation for the $260.7 \to 1111.8$ keV cascade in ^{136}I.

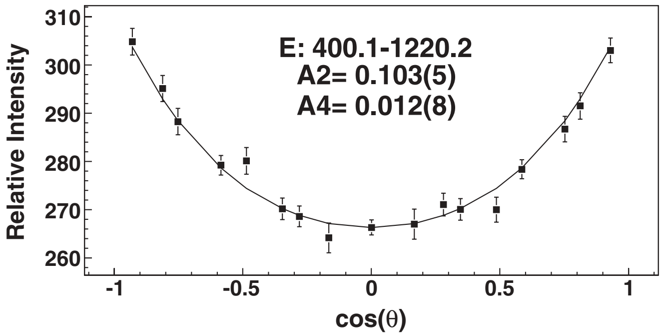

FIG. 4. Angular correlation for the 400.1 → 1220.2 keV cascade in ^{137}Xe. No attenuation is observed.

of the $E2$ 311.7 keV transition and the yrast 1046.6 keV transition, we conclude that the 1046.6 keV transition is of $E2$ character as well. Thus $23/2^-$ is assigned to the 2981.1 keV level, populating the $19/2^-$ level of energy at 1934.5 keV. We are also able to assign $27/2^-$ to the 3292.8 keV level according the preceding discussion. The assignments of $23/2^-$ to the 2981.1 keV level and $27/2^-$ to the 3292.8 keV level are consistent with the previous tentative experimental results [14] as well as theoretical prediction [17].

For ^{138}Cs, Li *et al.* [15] measured the angular correlation for the 1156.9 → 174.5 keV cascade, using the same method as in the present work, to be $A_2 = -0.07(1)$ and $A_4 = -0.02(2)$, which is consistent with theoretical A_2 and A_4 values for a pure quadrupole → pure dipole ($9^- \rightarrow 7^- \rightarrow 6^-$) cascade, as predicted by shell-model calculations [15]. However, the angular correlation results cannot exclude some quadrupole mixing. Here the correlation of the 185.5 → 1156.9 keV cascade is obtained as $A_2 = -0.076(23)$ and $A_4 = -0.007(34)$ in Fig. 7. With the known multipolarity of the 1156.9 keV transition ($E2$), the multipolarity of the 185.5 keV transition is assigned mainly $M1$ because this result agrees very well with shell-model calculations in Refs. [15,16] and the present calculation that predicts the spin and parity of the 1596.8 keV level to be 10^-. $E1$ assignment is not excluded experimentally, but it disagrees with the theory.

IV. SHELL-MODEL INTERPRETATION

In this section, we shall give a shell-model interpretation of the level schemes of the $N = 83$ isotones observed in

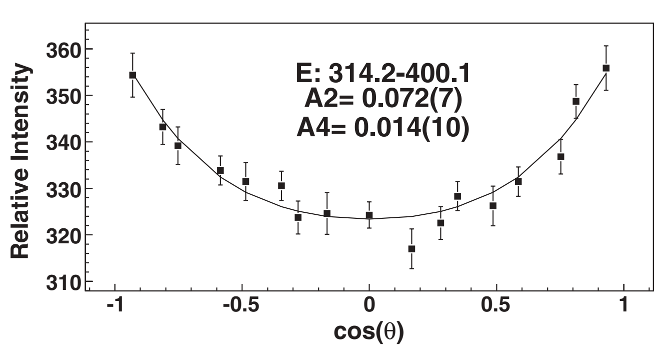

FIG. 5. Angular correlation for the 314.2 → 400.1 keV cascade in ^{137}Xe. An attenuation is observed.

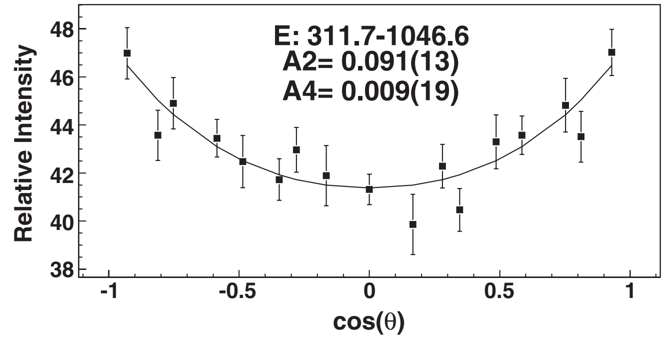

FIG. 6. Angular correlation for the 311.7 → 1046.6 keV cascade in ^{137}Xe.

the present experiment. The levels of ^{135}Te, ^{136}I, ^{137}Xe, and ^{138}Cs shown in Fig. 1 will be discussed, focusing attention on changes in the wave functions induced by the valence neutron beyond $N = 82$ as well as by the increase in the number of protons. To investigate this issue, we also discuss the level schemes of the corresponding $N = 82$ nuclei.

As in previous calculations, the valence neutron is assumed to occupy the six levels $1f_{7/2}$, $2p_{3/2}$, $0h_{9/2}$, $2p_{1/2}$, $1f_{5/2}$, and $0i_{13/2}$ of the 82–126 shell, while for protons, the model space includes the five levels $0g_{7/2}$, $1d_{5/2}$, $1d_{3/2}$, $2s_{1/2}$, and $0h_{11/2}$ of the 50–82 shell.

The Hamiltonian, which is the same as that of the previous shell-model studies on ^{132}Sn neighbors by the Napoli group [19–22], contains a two-body effective interaction derived from the CD-Bonn nucleon-nucleon potential [23]. The strong short-range repulsion of the latter is renormalized by constructing a smooth low-momentum potential $V_{\text{low-}k}$ [24], that is, it is used directly as input for the calculation of the effective interaction within the framework of the $\hat{Q}$-box folded-diagram expansion [25]. Details on the derivation of the two-body effective interaction as well as on the adopted single-proton and single-neutron energies can be found in Refs. [19,21], respectively. The shell-model calculations have been performed using the OXBASH computer code [26].

The experimental and calculated levels of ^{135}Te and ^{137}Xe are compared in Fig. 8, where we also report their parent states in ^{134}Te and ^{136}Xe. With respect to the levels of Fig. 1, we have

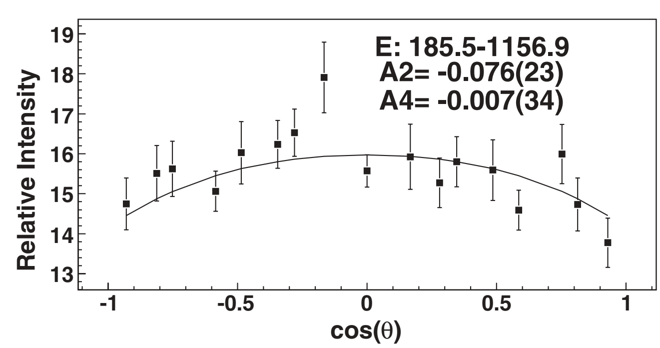

FIG. 7. Angular correlation for the 185.5 → 1156.9 keV cascade in ^{138}Cs.

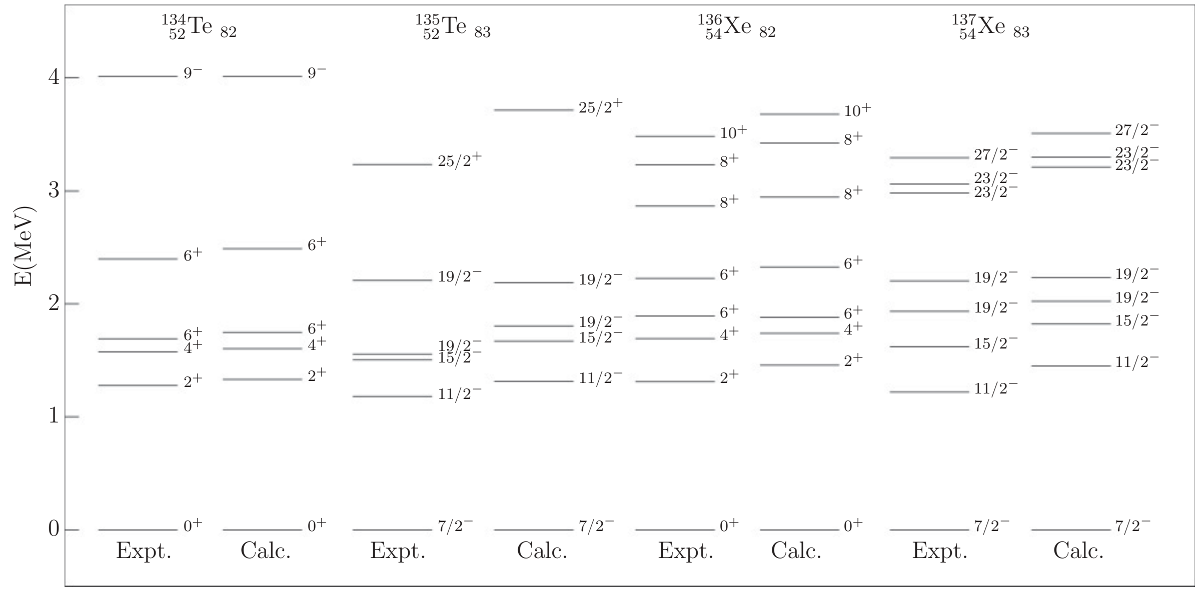

FIG. 8. Experimental and theoretical level schemes in ^{134}Te, ^{135}Te, ^{136}Xe, and ^{137}Xe. Data are taken from Refs. [2,11,12,14,27,28] and the present work.

added the second $19/2^-$ state to ^{135}Te and the second $19/2^-$ and $23/2^-$ states to ^{137}Xe [12,14].

We start discussion by noting the close correspondence between the level structures of ^{134}Te and ^{135}Te. As a matter of fact, from our calculation, it turns out that the states of ^{135}Te result essentially from the maximum spin alignment of an $f_{7/2}$ neutron with the 0^+, 2^+, 4^+, 6^+_1, 6^+_2, and 9^- states of ^{134}Te, which are all dominated by a single configuration. More precisely, the lowest four states of ^{134}Te arise from the $\pi(g_{7/2})^2$ configuration, while the 6^+_2 and 9^- states arise from the $\pi g_{7/2}d_{5/2}$ and $\pi g_{7/2}h_{11/2}$ configurations, respectively. The different natures of the two 6^+ states are confirmed by the different values of the measured half-lives[1]: 164.1(9) ns for the first and an upper limit of 16 ps for the second. Our calculated values, 185 ns and 2 ps, are in good agreement with experimental values. As for the $19/2^-$ states, which are found to preserve the proton structure of the two 6^+ states, only the half-life of the lowest one has been measured, and its value is 0.511(20) μs—rather close to that of the first 6^+ state. The calculated half-life, 0.595 μs, compares well with the experimental value. For the second $19/2^-$ state, a value on the order of a picosecond is predicted, which is consistent with the half-life of the second 6^+ state. The $E2$ transition rates have been calculated using effective proton and neutron charges of $1.55e$ and $0.7e$ [29], while the $M1$ transition rates were calculated with an effective $M1$ operator, which accounts for core-polarization effects [29]. The γ-ray energies were taken from experiment.

It is worth mentioning that the presence of an additional neutron in ^{135}Te favors configuration mixing. In fact, we find that the wave functions of the states in ^{134}Te have a percentage of dominant configuration ranging from 80% to 100%, while these limits become 74% and 82% for ^{135}Te.

As regards the agreement between experimental and calculated excitation energies, we find that the energies of ^{134}Te are very well reproduced, while for ^{135}Te, we predict a slightly expanded spectrum with a somewhat larger discrepancy for the $25/2^+$ state.

^{136}Xe and ^{137}Xe have an additional pair of protons with respect to the Te isotopes discussed earlier. This is reflected in ^{136}Xe by the presence of seniority-four states just above the second 6^+ state. These 8^+_1, 8^+_2, and 10^+ states arise mainly from the $\pi(g_{7/2})^4$, $\pi(g_{7/2})^3d_{5/2}$, and $\pi(g_{7/2})^2(d_{5/2})^2$ configurations, respectively, with a percentage of minor components less than 9%. The structures of the lowest five states in ^{136}Xe are quite similar to those of the corresponding states in ^{134}Te, with two additional protons in the $g_{7/2}$ level. However, the wave functions of the ^{136}Xe states have greater configuration mixing, the percentage of the dominant component ranging from 55% to 79%.

As was the case for ^{135}Te, we find that each level of ^{137}Xe in Fig. 8 results from the maximum spin alignment of an $f_{7/2}$

TABLE II. Wave functions of the two 6^+ states in ^{136}Xe and the two $19/2^+$ states in ^{137}Xe (components with a percentage smaller than 10% are omitted).

Nucleus	J^π	Configuration	Probability
^{136}Xe	6^+_1	$\pi(g_{7/2})^4$	77
	6^+_2	$\pi(g_{7/2})^3d_{5/2}$	79
^{137}Xe	$(\frac{19}{2}^+)_1$	$\pi(g_{7/2})^4\nu f_{7/2}$	30
		$\pi(g_{7/2})^3d_{5/2}\nu f_{7/2}$	44
	$(\frac{19}{2}^+)_2$	$\pi(g_{7/2})^4\nu f_{7/2}$	38
		$\pi(g_{7/2})^3d_{5/2}\nu f_{7/2}$	36

[1]Data extracted using the National Nuclear Data Center Online Data Service from the Evaluated Structure Data Files database; file revised as of October 1, 2009.

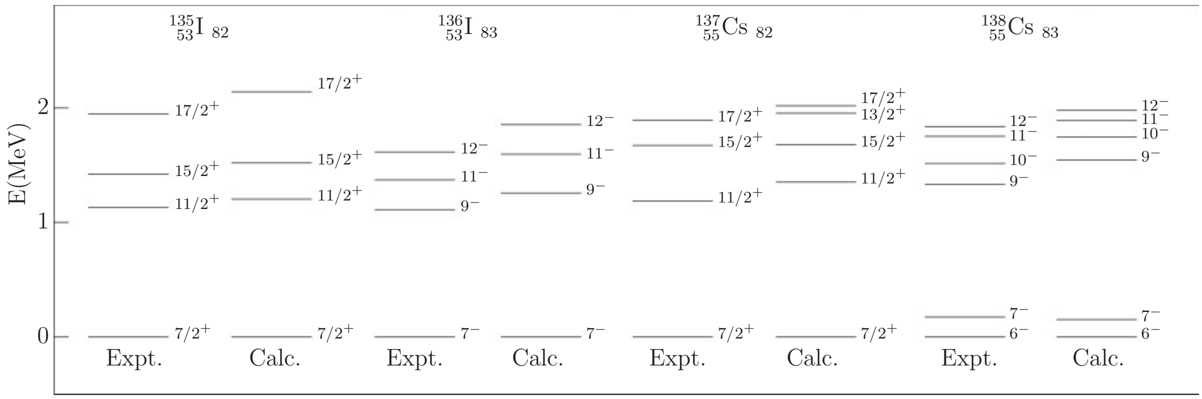

FIG. 9. Experimental and theoretical level schemes in ^{135}I, ^{136}I, ^{137}Cs, and ^{138}Cs. Data are taken from Refs. [11,13,15,16,27,28] and the present work.

neutron and a ^{136}Xe state, although here configuration mixing plays a more prominent role. This is particularly true for the two $19/2^-$ and two $23/2^-$ states. As an example, in Table II, we report the calculated wave functions of the two $19/2^-$ states together with those of the two 6^+ states in ^{136}Xe. We see that neither of the two states in ^{137}Xe preserves the simple proton structure of the 6^+ states, but they are both strongly mixed. The measured half-lives are consistent with these findings. The value measured [18] for the first $19/2^-$ state, 8.1(4) ns, is indeed different from the half-lives of the first and second 6^+ states, which are 2.95(9) μs and $\leqslant$50 ps, respectively. No experimental value is available for the second $19/2^-$ state. It is worth mentioning that our calculated half-lives for the 6^+ states in ^{136}Xe states are 1 μs and 13 ps, in agreement with experimental values. On the other hand, our value for the first $19/2^-$ state is an order of magnitude larger than the experimental value. However, assuming that the predicted ordering of the two $19/2^-$ states is not correct, the second calculated state would correspond to the first observed state with a calculated half-life of 7 ns which is quite close to the experimental value.

The calculated value of the g factor for the $15/2^-$ state in ^{137}Xe, which has been measured for the first time in this article, is +0.31, which agrees very well with the measured value $|g| = 0.26(5)$.

In Fig. 9, we show the calculated and experimental level schemes of ^{136}I and ^{138}Cs, together with those of the two corresponding $N = 82$ isotones. Note that for ^{136}I and ^{138}Cs, the spectra are not relative to the ground states but rather to the 7^- and 6^- isomeric states, respectively. It should be mentioned that some of the theoretical results for ^{136}I have been discussed in a recent article [30] by the Napoli group. There we focused on low-spin states with $J^\pi = 0^-$–7^- in connection with the evolution of the $\pi g_{7/2} \nu f_{7/2}$ proton-neutron multiplet, while here we confine ourselves to states populated in this experiment.

It turns out that the 7^-, 9^-, and 11^- states of ^{136}I are dominated by the $\pi(g_{7/2})^3 \nu f_{7/2}$ configuration with a percentage from 71% to 81%, while the 12^- state arises (99%) from the $\pi(g_{7/2})^2 d_{5/2} \nu f_{7/2}$ configuration. They all have the maximum J resulting from the coupling of an $f_{7/2}$ neutron to the $7/2^+$, $11/2^+$, $15/2^+$, and $17/2^+$ states of ^{135}I.

As for ^{137,138}Cs, they have been the subject of our study in Ref. [15], where high-spin-level energies were measured and compared with results of a shell-model calculation using the same Hamiltonian as in this article. Therefore we only focus here on a few points relevant to our discussion. Unlike ^{136}I, the γ cascade in ^{138}Cs starts from the 11^- state rather than the 12^- state. Actually, as shown in Fig. 9, the 12^- yrast state in ^{138}Cs has been located [15] at about 100 keV above the 11^- state, and the calculated 12^- energy is in very good agreement with the experimental value. The 11^- state decays to the 10^- state, which arises from the maximum spin alignment of an $f_{7/2}$ neutron and the yrast $13/2^+$ state in ^{137}Cs. The latter, which is still missing in the experimental spectrum, is predicted at 1.95 MeV excitation energy with a wave function composed mainly of the $\pi(g_{7/2})^4 d_{5/2}$ configuration. It is worth mentioning that in ^{136}I, we find a 10^- state that does not have an experimental counterpart; rather, it is only a few tens of kilo-electron-volts above the 11^- state. We calculate for the probability of the $E2$ transition $12^- \rightarrow 10^-$, a value that is more than 2 orders of magnitude smaller than the value of the $M1 + E2$ transition $12^- \rightarrow 11^-$.

Finally, we see that the two γ cascades in ^{136}I and ^{138}Cs end in two different isomeric states. For ^{136}I, the position of the 6^- state is unknown and the position of the 7^- state with respect to the ground state is still controversial [31,32]. The nonobservation of the 6^- state in this experiment may imply that it lies either above the 7^- state or very close to it. Our calculations support the second alternative, which says that the 6^- state is predicted at 30 keV below the 7^- state.

V. CONCLUSION

The knowledge of g factors in isotopes with several nucleons outside the doubly magic core ^{132}Sn is extended in this article with the first measurement of the g factor of the $15/2^-$ state in ^{137}Xe. Our result is in good agreement with shell-model calculations. On the basis of observed angular correlations, spins and parities are assigned to several levels in the $N = 83$ isotones ^{135}Te, ^{136}I, ^{137}Xe, and ^{138}Cs. These assignments are in agreement with the previous experimental results and shell-model predictions.

ACKNOWLEDGMENTS

The work at Vanderbilt University, Mississippi State University, University of Tennessee, and Lawrence Berkeley National Laboratory is supported by the US Department of Energy under Grant and Contract Nos. DE-FG05-88ER40407, DE-FG02-95ER40939, DE-FG02-96ER40983, and DE-AC03-76SF00098. The work at Tsinghua University is supported by the National Natural Science Foundation of China under Grant Nos. 10775078 and 10975082 and by the Major State Basic Research Development Program under Grant No. 2007CB815005.

[1] A. V. Daniel *et al.*, Nucl. Instrum. Methods Phys. Res. B **262**, 399 (2007).
[2] Y. X. Luo *et al.*, Phys. Rev. C **64**, 054306 (2001).
[3] R. M. Steffen and K. Alder, in *The Electromagnetic Interaction in Nuclear Spectroscopy*, edited by W. D. Hamilton (Elsevier, New York, 1975).
[4] E. Matthias, S. S. Rosenblum, and D. A. Shirley, Phys. Rev. Lett. **14**, 46 (1965).
[5] H. W. Taylor, B. Singh, F. S. Prato, and R. McPherson, At. Data Nucl. Data Tables **9**, 1 (1971).
[6] P. E. Haustein, H. W. Taylor, R. McPherson, and R. Fairchild, At. Data Nucl. Data Tables **10**, 321 (1972).
[7] C. Goodin *et al.*, Phys. Rev. C **78**, 044331 (2008).
[8] C. Goodin, J. R. Stone, N. J. Stone, A. V. Ramayya, A. V. Daniel, J. H. Hamilton, K. Li, J. K. Hwang, G. M. Ter-Akopian, and J. O. Rasmussen, Phys. Rev. C **79**, 034316 (2009).
[9] C. Goodin *et al.*, Phys. Rev. C **80**, 014318 (2009).
[10] G. N. Rao, Hyperfine Interact. **26**, 1119 (1985).
[11] P. Bhattacharyya *et al.*, Phys. Rev. C **56**, R2363 (1997).
[12] B. Fornal *et al.*, Phys. Rev. C **63**, 024322 (2001).
[13] W. Urban, M. Saha Sarkar, S. Sarkar, T. Rząca-Urban, J. L. Durell, A. G. Smith, J. A. Genevey, J. A. Pinston, G. S. Simpson, and I. Ahmad, Eur. Phys. J. A **27**, 257 (2006).
[14] P. J. Daly *et al.*, Phys. Rev. C **59**, 3066 (1999).
[15] K. Li *et al.*, Phys. Rev. C **75**, 044314 (2007).
[16] T. Rząca-Urban, W. Urban, J. L. Durell, M. Saha Sarkar, S. Sarkar, J. L. Durell, A. G. Smith, B. J. Varley, and I. Ahmad, Eur. Phys. J. A **27**, 257 (2006).
[17] S. Sarkar and M. S. Sarkar, Phys. Rev. C **64**, 014312 (2001).
[18] R. G. Clark, L. E. Glendenin, and W. L. Talbert, in *Proceedings of the Third IAEA Symposium on the Physics and Chemistry of Fission, Rochester, 1973* (International Atomic Energy Agency, Vienna, 1974), Vol. 2, p. 221.
[19] L. Coraggio, A. Covello, A. Gargano, and N. Itaco, Phys. Rev. C **72**, 057302 (2005).
[20] L. Coraggio, A. Covello, A. Gargano, and N. Itaco, Phys. Rev. C **73**, 031302(R) (2006).
[21] A. Covello, L. Coraggio, A. Gargano, and N. Itaco, Prog. Part. Nucl. Phys. **59**, 401 (2007).
[22] A. Gargano, L. Coraggio, A. Covello, and N. Itaco, J. Phys. Conf. Ser. **168**, 012013 (2009).
[23] R. Machleidt, Phys. Rev. C **63**, 024001 (2001).
[24] S. Bogner, T. T. S. Kuo, L. Coraggio, A. Covello, and N. Itaco, Phys. Rev. C **65**, 051301(R) (2002).
[25] L. Coraggio, A. Covello, A. Gargano, N. Itaco, and T. T. S. Kuo, Prog. Part. Nucl. Phys. **62**, 135 (2009).
[26] B. A. Brown, A. Etchegoyen, and W. D. M. Rae, Michigan State University National Superconducting Cyclotron Laboratory Report No. 524 (1988).
[27] C. T. Zhang *et al.*, Phys. Rev. Lett. **77**, 3743 (1996).
[28] S. K. Saha *et al.*, Phys. Rev. C **65**, 017302 (2001).
[29] A. Korgul *et al.*, Eur. Phys. J. A **32**, 25 (2007).
[30] L. Coraggio, A. Covello, A. Gargano, and N. Itaco, Phys. Rev. C **80**, 021305(R) (2009).
[31] W. Urban *et al.*, Eur. Phys. J. A **27**, 257 (2006).
[32] B. Fogelberg, K. A. Mezilev, V. I. Isakov, K. I. Erokhina, H. Mach, E. Ramstrom, and H. Gausemel, Phys. Rev. C **75**, 054308 (2007).